Deepcell

High-dimensional morphology analysis with the REM-I platform reveals subtle morphological changes during cell death

Highlights

- Technological advances in AI have enabled cell biology to be explored on a high-dimensional level.
- The REM-I platform leverages AI to capture distinct morphological traits associated with the complex and dynamic process of cell death.
- The REM-I platform combined with its Human Foundation Model displays the discriminative resolution necessary to identify subtle changes apparent in very early phase and mid-phase apoptosis.
- Deep learning and computer vision derived morphological features provide orthogonal biological information to not only complement, but also reveal more than traditional cytotechnology and protein-based biomarker analysis can achieve.

Graphical abstract: characterizing cell health

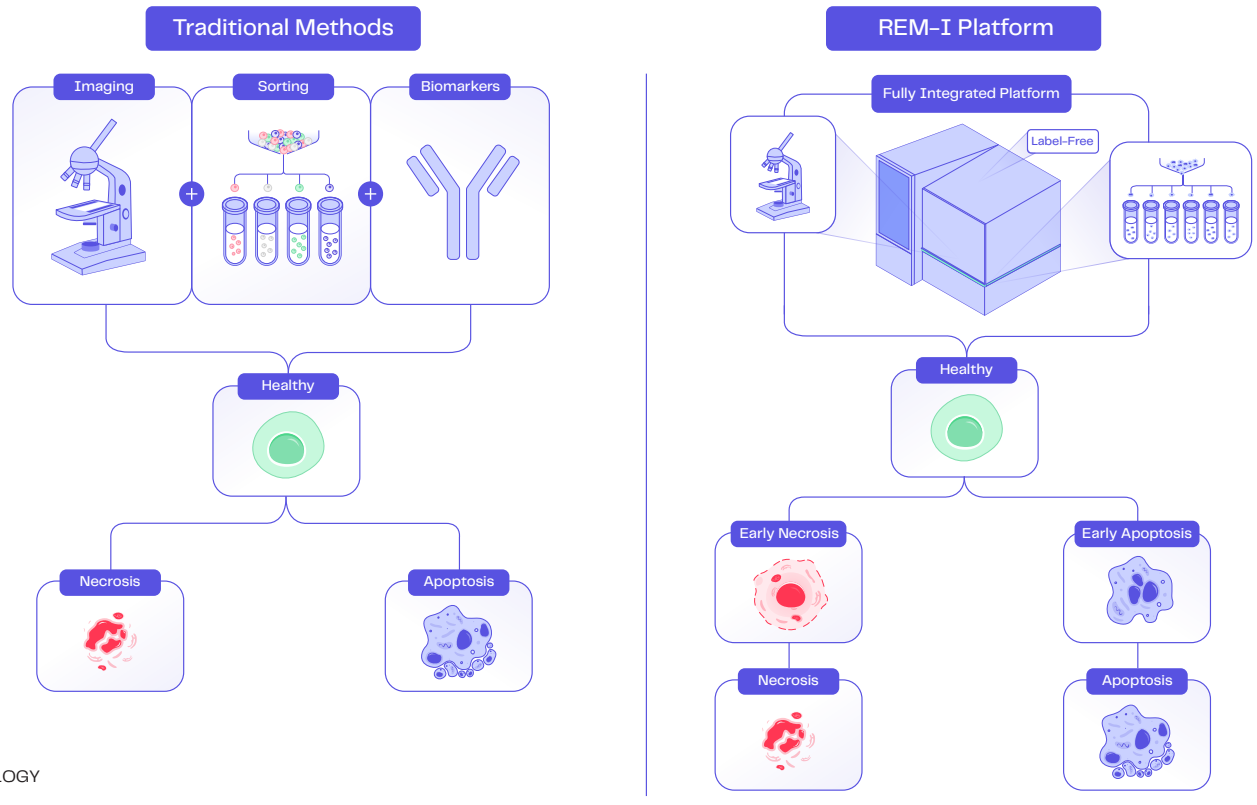

Introduction

Morphology is a fundamental cell property associated with cell identity, state, function, and disease. Current methods to quantify cell morphology are limited to a small number of parameters (such as cell granularity and cell size) or to a set of 4 or 5 molecular markers, which result in irreversible cell alterations, preventing further downstream functional studies to occur. In particular, Annexin V is a common detection method for early apoptosis as it binds to exposed phosphatidylserine, a marker of apoptosis, on the outer leaflet of the plasma membrane. SYTOX AADvanced is a marker for late stage apoptosis and necrosis as it binds to the nucleus after cells have lost membrane integrity and progressed into later stages of cell death.

In this application note, we show that high-dimensional morphology profiling by the REM-I platform not only complements and correlates with traditional, established molecular cell characterization tools (e.g., flow cytometry), but also represents an important descriptor for complex, dynamic biological processes. Our approach applies deep learning and computer vision to characterize cells in a label-free manner based on real-time interpretation of high-content morphology data. The REM-I platform combines microfluidics and high-speed imaging in the REM-I instrument, deep learning and computer vision in our Human Foundation Model (HFM), and data analysis and visualization in our Axon data suite (Figure 1). The REM-I workflow begins with single cell suspensions of human cells, such as patient-derived immune cells, cell lines, or dissociated tissues, being loaded onto the REM-I instrument to generate high-resolution images (0.16 um/pixel), which serve as raw data input to our AI model. As the label-free cells flow through the microfluidic channel, high-resolution brightfield images are captured and sent to the HFM for characterization and identification in real-time (Figure 2).

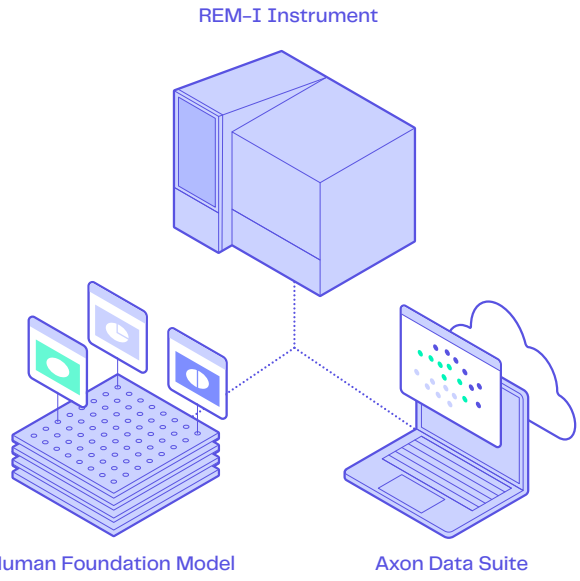

Figure 1. *Components of the REM-I platform. The REM-I platform consists of the REM-I instrument for imaging and sorting, the Human Foundation Model for real-time cell characterization, and the Axon data suite for data visualization and analysis.*

Methods

To begin an experimental run, samples from established human cell lines or dissociated tissue biopsies in single cell suspension are loaded onto a microfluidic chip. Images of individual cells are captured and analyzed in real-time by a combined deep learning and morphometric (computer vision) foundation model to generate high-dimensional quantitative morphological profiles and guide subsequent cell sorting, if desired. Cell images are randomly sampled, features extracted, standardized, and projected into a lower dimensional PCA basis. Nearest neighbors are identified using Euclidean distance in PCA space, then these neighbors are used to identify leiden clusters and visualized on a 2D Uniform Manifold Approximation and Projection (UMAP).

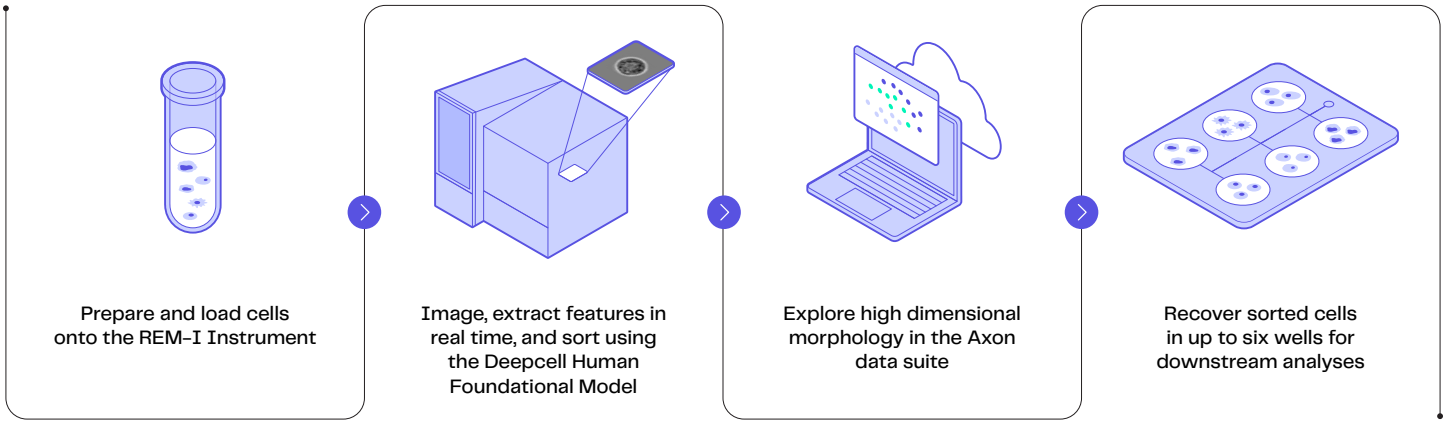

Figure 2. *REM-I platform workflow. Single cell suspensions are loaded onto a microfluidic chip for high-speed, high-resolution imaging. Images are analyzed in real-time by self-supervised deep learning via the Human Foundation Model to extract morphological features and inform sorting decisions based on predicted cell class. Data is stored and analyzed in the Axon data suite, while sorted cells of interest can be assayed further with molecular or functional studies.*

Imaging cell death and sample health

Jurkat E6-1 cells were cultured in RPMI-1640 medium with 10% fetal bovine serum (FBS) at 37°C with 5% CO_2. Cells were passaged routinely and suspension cells were prepared at 2 x 10^6 cells/ mL for apoptosis and necrosis induction. The following treatments were used to induce apoptosis or necrosis, as previously reported (Figure 3):

- Staurosporine (ab120056, Abcam), a protein kinase inhibitor, was administered to live Jurkat cells at a final concentration of 2 µM and incubated at 37°C with 5% CO_2 for 3 hrs or 18 hrs to induce apoptosis by G_2/M cell cycle arrest [1].
- Camptothecin (ab120115, Abcam), a DNA topoisomerase inhibitor, was administered to live Jurkat cells at a final concentration of 20 µM and incubated at 37°C with 5% CO_2 for 5 hr to induce apoptosis by perturbing topoisomerase I [2-3].
- Heat shock at 70°C for 5 min was used to induce primary necrosis, protein degradation, and loss of mitochondrial membrane potential [4].

Following treatment, cells were split into two aliquots for simultaneous REM-I morphology profiling and flow cytometry assessment. For morphology profiling experiments, 3 x 10^6 cells per mL in single cell suspension were run on the REM-I platform with a flow rate of ~300 cells/sec and >40,000 images were captured. Associated morphology data results can be accessed here: https://exploredata.deepcell.com/. For flow cytometry, 1 x 10^6 cells in 100 µL were incubated with 5 µL Pacific Blue™ Annexin V stock (per manufacturer recommendation) and 1 µl of SYTOX™ AADvanced™ (A35136, Thermo Fisher) for 30 minutes at room temperature and analyzed with BD FACSMelody™ Cell Sorter and BD FACSChorus™ Software (BD Biosciences, California).

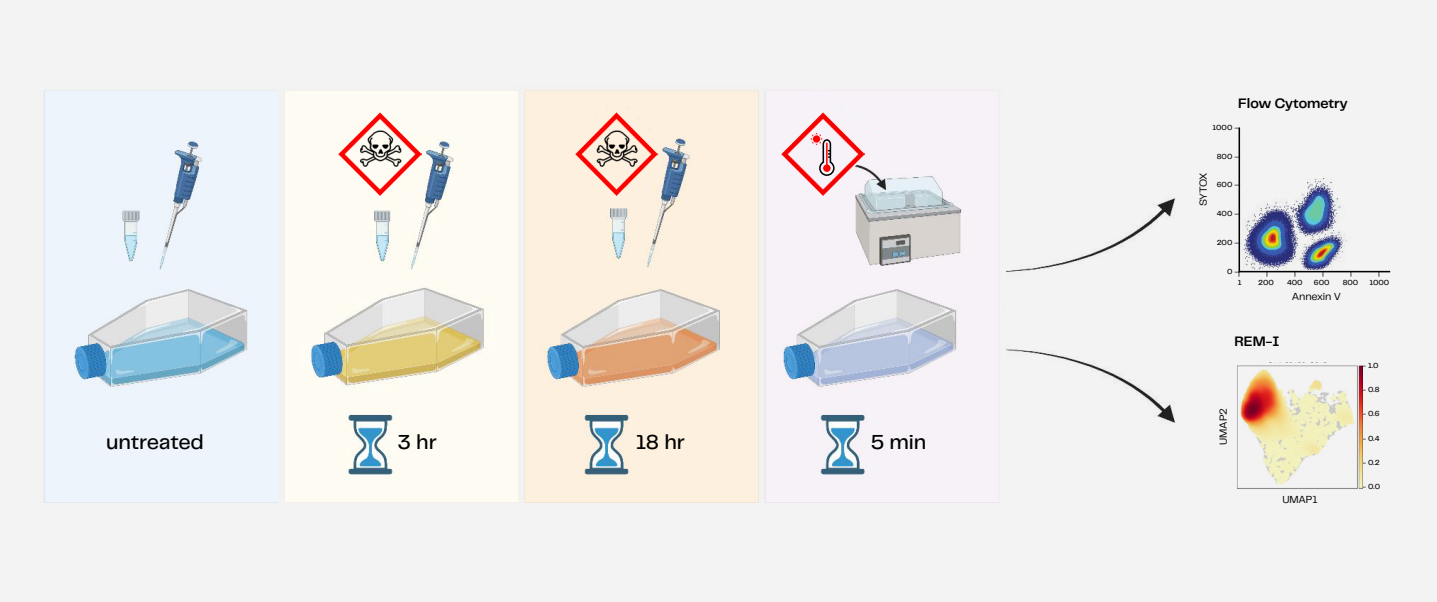

Figure 3. *Apoptosis and necrosis induction workflow. Staurosporine, camptothecin, and heat shock treatments were used to induce cell death in Jurkat cells. Samples were analyzed using flow cytometry and REM-I high-dimensional morphology analysis.*

Results

Characterization of complex cell morphology changes during apoptosis and necrosis

Aligning cell death morphotypes with known flow cytometry biomarkers

Morphological changes associated with alterations in cell state, health, and fitness have been reported in drug response, cell differentiation, and disease progression studies [5–6]. Specifically, apoptosis and necrosis processes are distinguished by a set of morphological and biochemical events such as externalization of phosphatidylserine, activation of caspases, and maintenance of plasma and lysosomal membrane integrity. The ability to profile sample health at scale can be costly, time consuming, and labor intensive. In addition, the later stages of apoptosis exhibit significant cell degradation, leading to smaller apoptotic cells possibly being mistaken for debris. Here, we utilized label-free, high-dimensional morphology profiling of cells undergoing apoptosis and necrosis using deep learning to reveal novel cell characterization insights in response to cytotoxicity.

To identify unique morphological patterns ('morphotypes') across the necrosis and apoptosis continuum, Jurkat T lymphocytes were induced with known apoptosis and necrosis treatments and simultaneously analyzed with the REM-I platform and flow cytometry. Notably, healthy/viable cells localize to the right side of the UMAP, while cells undergoing cell death and cell debris localize to the left side of the UMAP (Figure 4).

High-dimensional morphology analysis detects subtle morphological changes not seen by flow cytometry during the stages of cell death

Analysis of high-dimensional morphology and flow cytometry results revealed that expected Annexin V and SYTOX staining levels correspond to respective cell death induction treatments and timing (Figure 5A). With flow cytometry results, Annexin V+/SYTOX- staining indicates apoptosis, Annexin V +/SYTOX+ staining indicates necrosis, Annexin V-/SYTOX+ indicates dead cells, and Annexin V-/SYTOX- staining indicates viable healthy cells (Figure 5A). Morphological profiling showed untreated, apoptotic, and necrotic cells exhibited separate morphotypes, with respective cell death stages localizing to distinct embedding

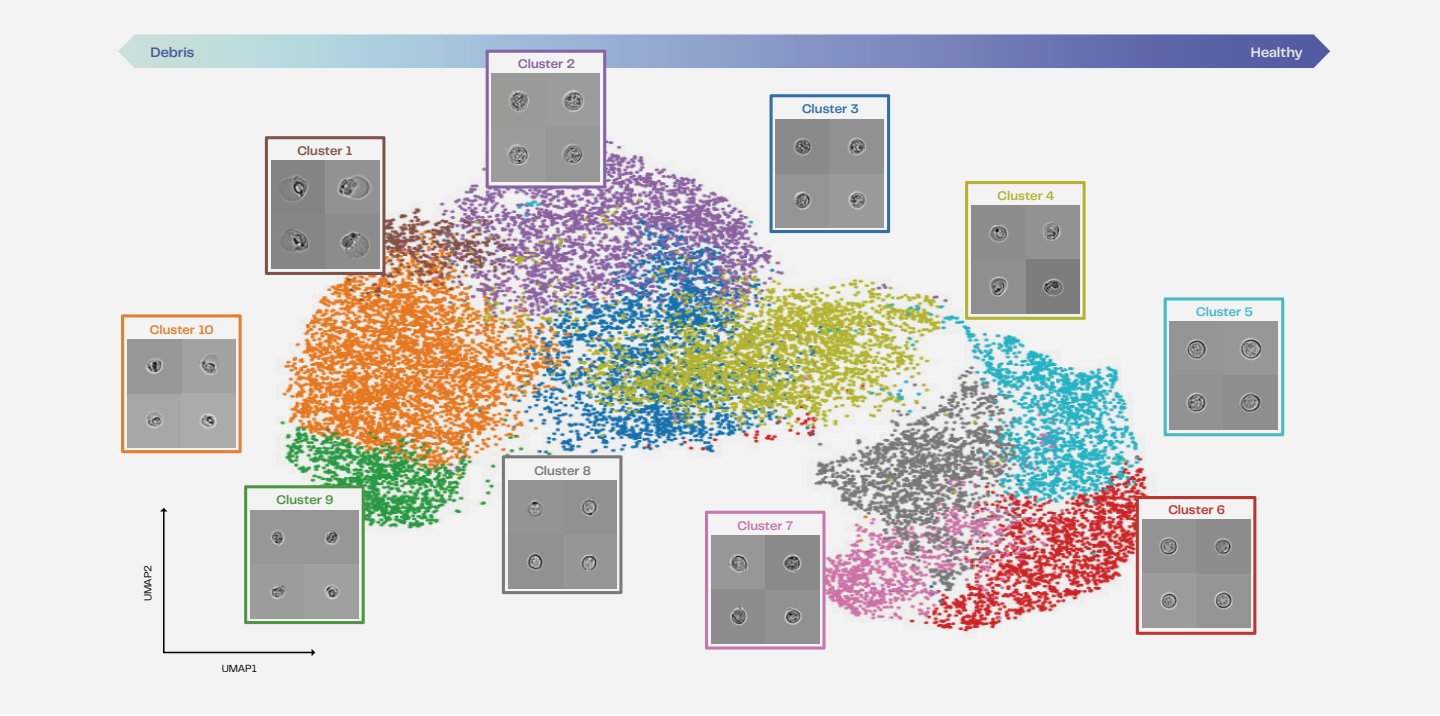

Figure 4. *Morphology UMAP from the REM-I platform of cells undergoing apoptosis and necrosis. (A) Morphology UMAP generated by the REM-I platform and colored by cluster computed using the Leiden algorithm, with randomly chosen representative images from each cluster shown. Leiden cell clusters correlate with shifts in morphology as cells progress through apoptosis and necrosis. Scale bar indicates 10 µm.*

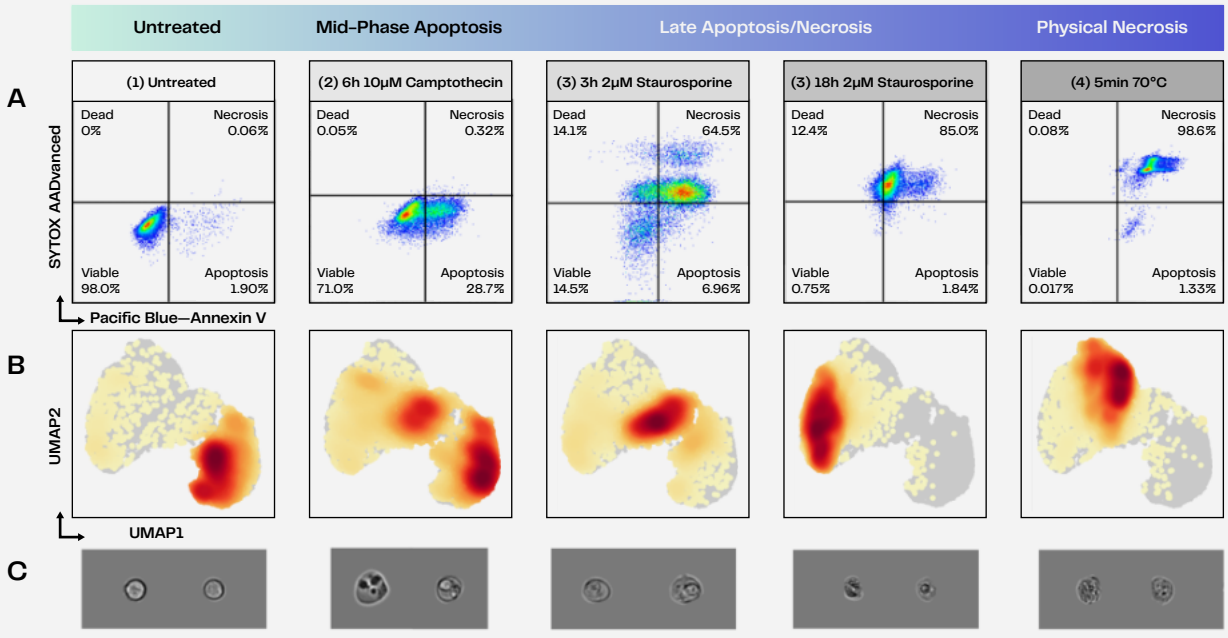

Figure 5. *REM-I detects subtle morphological changes not seen by flow cytometry during the stages of cell death. Cell death was induced in Jurkat T lymphocytes with indicated treatments. (A) Flow cytometry profiles show percentage of viable, dead, apoptotic, and necrotic cell populations based on membrane stains (Annexin V) and DNA intercalator (SYTOXTM). Single cell events are displayed. (B) UMAP visualization of 115 HFM dimensions were generated following imaging on REM-I and colored by population density. (C) Representative images from the REM-I platform of each condition. Cells in various health and death pathways cluster separately based on morphology.*

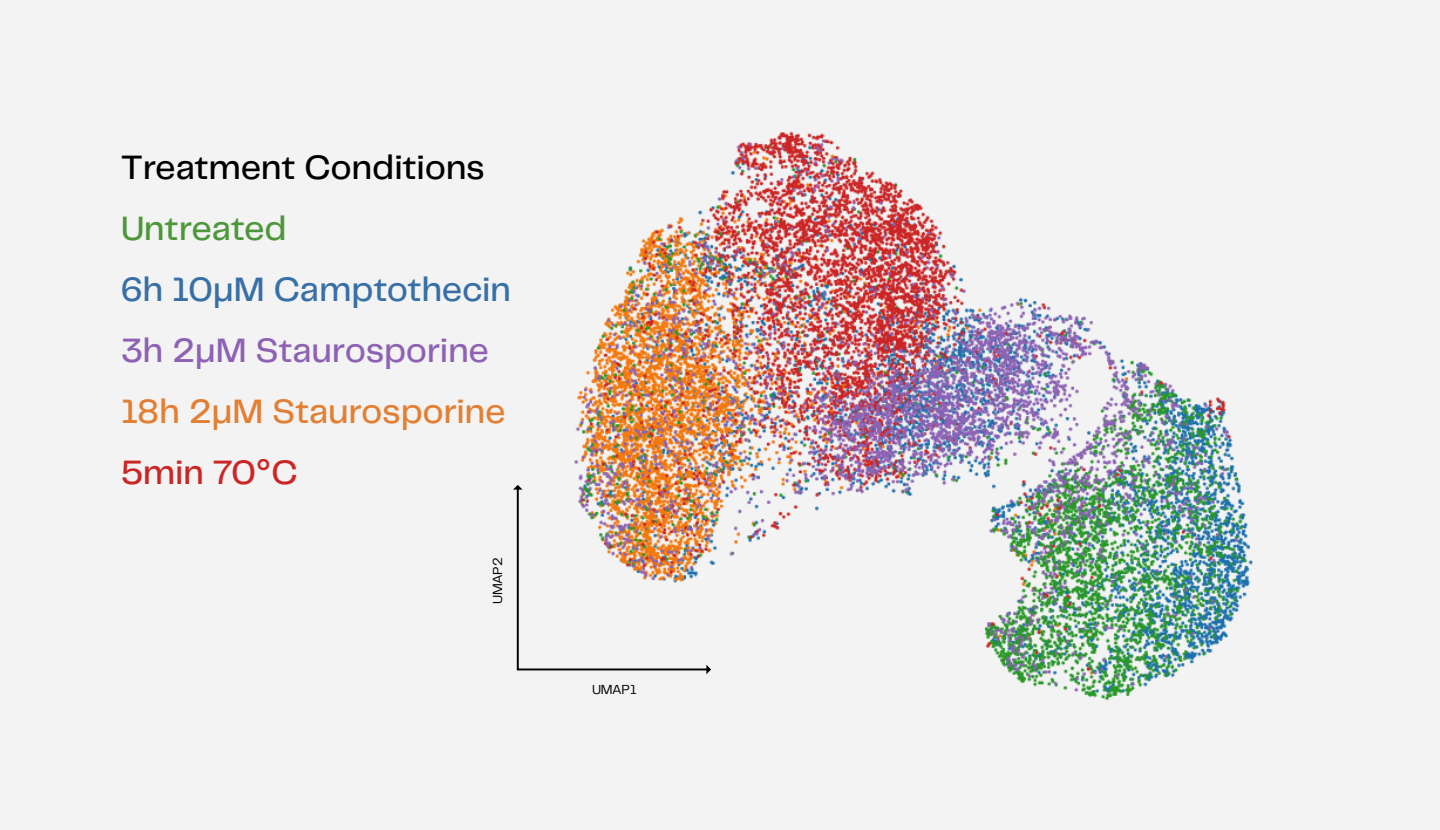

Figure 6. *Cell death induction results in consistent morphological shifts. Upon treatment with camptothecin (mid-phase apoptosis inducer), staurosporine (late stage apoptosis/necrosis inducer), and heat shock (physical necrosis inducer), cells exhibit consistent morphological alterations based on the perturbation.*

Figure 7. *REM-I images capture classic visual cues of cell viability status. REM-I morphological profiling recapitulates "ground truth" by capturing known morphological shifts associated with apoptotic and necrotic progression.*

space (Figure 5B). Specifically, as untreated (healthy) cells progress to mid-phase apoptosis then late stage apoptosis/necrosis, morphological profiles shift from right to left along UMAP dimension 1 (Figure 5A-C). Flow cytometry, relying on the two common biomarkers, Annexin V and SYTOX, appear to lack the discriminative resolution necessary to identify subtle changes apparent in very early phase/stressed cell stage and mid-phase apoptosis. For example, mid-phase apoptosis induced by a 6 h treatment with 10 µM camptothecin resulted in a morphological shift in the main population, with a majority of cells localizing to different areas of the morphology UMAP compared to healthy cells. By contrast, flow cytometry analysis showed the main population still stained as healthy Annexin V-/SYTOX- (71% viable) (Figure 5A-B). These results suggest that high-dimensional morphology analysis can capture subtle biological changes in cells even at very early time points of apoptosis. This also indicates each cell treatment condition assayed in our study is associated with distinct changes in morphological traits, as quantified by 115 dimensions. Notably, cells occupying the same flow cytometry gate segregate in distinct clusters based on morphological traits, indicating ability of high-dimensional morphology to resolve and/or identify subtle morphological changes during the complex and dynamic biological process of cell death.

Concordance between REM-I captured morphological features and cytology analysis

Morphological features associated with apoptosis include cell shrinkage, nuclear condensation, formation of apoptotic bodies, large clear vacuoles, and blebbing [5, 8-10]. These distinct morphological features associated with apoptosis progression can be seen with REM-I high-resolution brightfield images. Notably, each treatment condition performed was associated with localized cell clusters (Figure 6), indicating each treatment condition corresponds to reproducible and consistent alterations captured by morphological signatures.

While 115 features were used for high-dimensional analysis, numerous morphological traits detectable by eye recapitulate classical visual cues used by cytologists to distinguish stages of cell death. Nuclear condensation begins with "ring" shaped formation, then "necklace" shaped formation, and finally nuclear collapse and disassembly [9-10]. Following these steps the apoptotic bodies begin to form, typically dividing organelles, nuclear remnants, and cytoplasm [5]. These established features were recapitulated in REM-I images with both staurosporine and camptothecin treatments (Figure 7).

Using high-dimensional morphology data generated on the REM-I platform, we observed morphological shifts characterizing apoptosis and necrosis. The combination of deep learning and computer vision derived features extracted by the HFM enabled insight into the morphological trajectory of cell death. These results were aligned with flow cytometry results that relied on Annexin V and SYTOX to characterize healthy, apoptotic, necrotic, and dead cell populations. Additionally, morphological data captured subtle changes occurring in early apoptosis and stressed cells that were not clear from biomarker staining alone. Lastly, high-resolution brightfield images captured on the REM-I instrument recapitulate known visual features used by cytologists to determine cell death, affirming the strength of using morphological data to characterize complex cell processes.

Conclusion

- The REM-I platform combines label-free imaging, deep learning, computer vision, and gentle cell sorting to harness high-dimensional single cell morphology as a quantitative biological readout.
- As cells progress through apoptosis and necrosis, morphological traits captured by REM-I correspond with traditional visual analysis of cell death.
- In addition to concordance with traditional cell death detection techniques (Annexin V and SYTOX staining), high-dimensional morphology profiling has added value of detecting subtle morphological changes during distinct stages of cell death.

Resources

Analyze high-dimensional morphology enabled by self-supervised deep learning by exploring the following datasets at https://exploredata.deepcell.com/.

- → Identification of cancer cells
- → Exploration of cancer cell subpopulations
- → Investigation of immune cell diversity in tumor microenvironment
- → Imaging of cell death pathways in Jurkat cells
- → Morphological profiling of Human Adult Stem Cells

References

1. Antonsson, A. & Persson, J. L. Induction of Apoptosis by Staurosporine Involves the Inhibition of Expression of the Major Cell Cycle Proteins at the G_2/M Checkpoint Accompanied by Alterations in Erk and Akt Kinase Activities. Anticancer Research 29, 2893–2898 (2009).
2. Li, F., Jiang, T., Li, Q. & Ling, X. Camptothecin (CPT) and its derivatives are known to target topoisomerase I (Top1) as their mechanism of action: did we miss something in CPT analogue molecular targets for treating human disease such as cancer? Am J Cancer Res 7, 2350–2394 (2017).
3. Tesauro, C. et al. Topoisomerase I activity and sensitivity to camptothecin in breast cancer-derived cells: a comparative study. BMC Cancer 19, 1158 (2019).
4. Janko, C. et al. Navigation to the graveyard–induction of various pathways of necrosis and their classification by flow cytometry. Methods Mol Biol 1004, 3–15 (2013).
5. Elmore, S. Apoptosis: a review of programmed cell death. Toxicol Pathol 35, 495–516 (2007).
6. Hwang, D. W. & Lee, D. S. Optical imaging for stem cell differentiation to neuronal lineage. Nucl Med Mol Imaging 46, 1–9 (2012).
7. Traag, V. A., Waltman, L. & van Eck, N. J. From Louvain to Leiden: guaranteeing well-connected communities. Scientific Reports 9, 5233 (2019).
8. Bottone, M. G. et al. Morphological Features of Organelles during Apoptosis: An Overview. Cells 2, 294–305 (2013).
9. Rello, S. et al. Morphological criteria to distinguish cell death induced by apoptotic and necrotic treatments. Apoptosis 10, 201–208 (2005).
10. Toné, S. et al. Three distinct stages of apoptotic nuclear condensation revealed by time-lapse imaging, biochemical and electron microscopy analysis of cell-free apoptosis. Exp Cell Res 313, 3635–3644 (2007).

Contact us

INFO@DEEPCELLBIO.COM · DEEPCELL.COM

Deepcell